SURVEY AND LOGISTICS REPORT ON A HELICOPTER BORNE VERSATILE TIME DOMAIN ELECTROMAGNETIC (VTEM) SURVEY

on the

MOSKU AREAS

FINLAND

for

ANGLO AMERICAN EXPLORATION BV SUOMEN SIVULIIKE

by

GEOTECH AIRBORNE LIMITED

No. 12 Tigne Place, Office 2/1,
Tigne Street, Sliema,
SLM 3137, Malta
Office: +233-21-521-745
Fax: +27-11-312-2757
www.geotechairborne.com
e-mail: info@geotechairborne.com

Project A806
August, 2010

TABLE OF CONTENTS

APPENDICES

SURVEY AND LOGISTICS REPORT ON A HELICOPTER-BORNE VTEM SURVEY

1. SURVEY SPECIFICATIONS

1.1. General

Job Number	A806
Client	Anglo American Exploration BV Suomen Sivuliike.
Project Area	Mosku
Location	Finland
Number of Blocks	3 + A582 Mosku and kevitsa areas
Total line kilometres	1824km (A806 only)
Survey date	6 - 16 July , 2010
Client Representative	Jim Coppard, Exploration Manager for Europe Tel: +46 706351336 Mobile: +44 777 1664358 jcoppard@angloamerican.co.uk
Client address	c/o Anglo American Exploration BV PO Box 14 Mala, 93070, Sweden

1.2. VTEM flight plan on Google EARTH™ Background

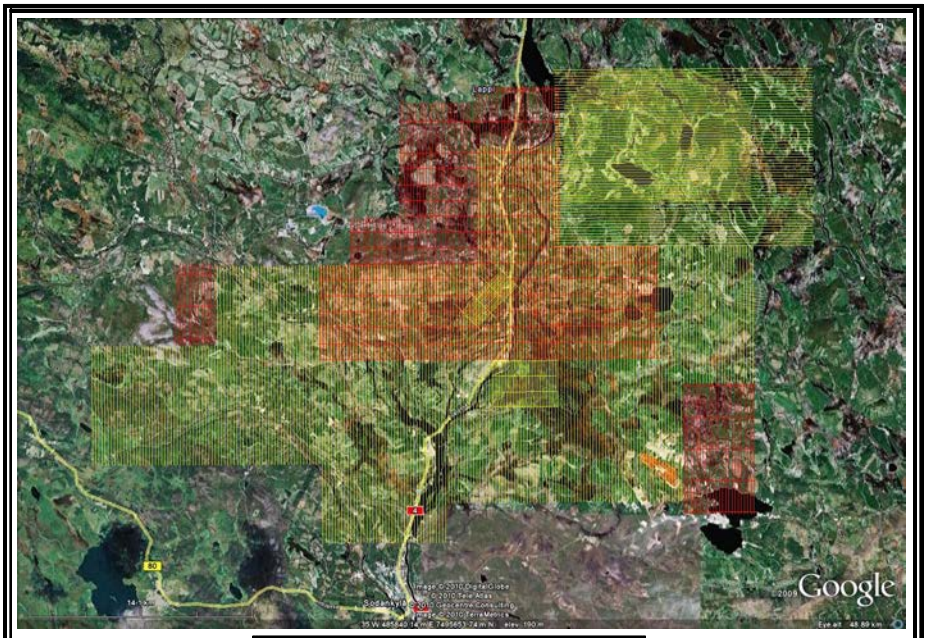

Anglo American Exploration BV Suomen Sivuliike
Mosku Areas 1 - 6,Finland
VTEM Flight Plans
Google Earth™ Background
Geotech Airborne Malta Limited

August 2010

* A806 in red and A582 in yellow

1.3. Survey block coordinates.

Easting UTM 35N	Northing UTM 35N
Mosku Blocks 1, 2, 4, 5 – A806	
476742.83	7493468.38
476742.83	7499366.03
478742.83	7499366.03
478742.83	7502367
481935.01	7502367
481935.02	7509661.91
486833.05	7509661.91
486833.05	7510661.5
492142.83	7510661.5
492142.83	7500515.55
498342.83	7500515.55
498428.41	7493468.35
476742.83	7493468.38
Mosku Block 3 – A806	
499942.83	7483572.3
504525.96	7483572.3
504525.97	7491868.98
499942.83	7491868.99
499942.83	7483572.3
Mosku Block 6 – A806	
467742.8	7494368
470142.8	7494368
470142.8	7499566
467742.8	7499566
467742.8	7494368
Mosku NS – A582	
462342.83	7494368.05
470339.63	7494368.03
470339.64	7499366.04
486833.05	7499366.01
486833.06	7506863.02
491831.06	7506863.01
491831.06	7500515.55
504326.08	7500515.55
504326.05	7491868.98
499827.85	7491868.99
499827.84	7484371.98
484833.83	7484372.01
484833.82	7481873
476837.02	7481873.02
476837.02	7486871.02
462342.81	7486871.04

Mosku EW – A582	
491831.05	7500515.55
508174.53	7500515.52
508174.54	7511860.99
491831.07	7511861.01
491831.05	7500515.55
Mosku 7 – A582	
485733.48	7496367.21
488332.45	7499066.13
489432.01	7497966.57
486833.04	7495467.57
485733.48	7496367.21
Mosku 8 – A582	
487842.64	7490369.61
487842.64	7493368.41
491842.64	7493368.4
491842.64	7490369.6
487842.64	7490369.61
Kevitsa – A582	
492410.5	7503315.55
492428.03	7509565.75
494708.75	7511771.67
499788.81	7511751.23
502858.86	7510889.04
504240.1	7509303.29
504214.67	7503315.55
492410.5	7503315.55

1.4. Survey block specifications

Survey block	Line spacing (m)	Line-km (Contract)	Line-km (delivered)	Flight direction	Line numbers
Mosku 1, 2, 4, 5	200	1522	1532	000°- 180°	L50010 – L51080
	1000/2000			090°- 270°	T95010 – T95180
Mosku 3	200	214	216	000°- 180°	L61010 – L61230
	2000			090°- 270°	T96110 – T96150
Mosku 6	200	75	76	000°- 180°	L60010 – L60131
	2000			090°- 270°	T96011 – T96031
Mosku_NS	200	2969	2991	000°- 180°	L20010 – L22110
	N/A			N/A	N/A
Mosku_EW & Kevitsa	200	932	1406	090°- 270°	L30010 – L30570
	N/A			N/A	N/A
Mosku 7	100	67	68	045°- 225°	L70010 – L70150
	1200			135°- 315°	T97010 – T97040
Mosku 8	200infills	79	81	000°- 180°	L81280 – L81480
	1000			090°- 270°	T98010 – T98040

1.5. Survey schedule

Date	Flight #	Block	Nominal Production Km flown	Comments
6-July-10	2	1,2,4,5	28.8	Production
7-July-10	3	1,2,4,5	143.6	Production
8-July-10	4,5,6	1-5	397.3	Production
9-July-10	N/A	N/A	N/A	Bad weather
10-July-10	7	1,2,4,5	112.9	Production
11-July-10	8,9,10	1,2,4,5	380.7	Production
12-July-10	11	1,2,4,5	48.8	Production
13-July-10	12,13	1,2,4,5,6	143.0	Production
14-July-10	14,15,16	1,2,4,5	241.8	Production
15-July-10	N/A	N/A	N/A	Pilot rest day
16-July-10	17,18,19	1,2,4,5,6	331.6	Production

2. SYSTEM SPECIFICATIONS

2.1. Instrumentation

Survey Helicopter	
Model	LAMA SA 315B
Registration	I-ICGR
Operating Company	AirWalser
Nominal survey speed	80 km/h
Nominal terrain clearance	80 m
VTEM Transmitter	
Coil diameter	26 m
Number of turns	4
Pulse repetition rate	25 Hz
Peak current	200 Amp
Duty cycle	36.74%
Peak dipole moment	435,362 NIA
Pulse width	7.35 ms
Nominal terrain clearance	46 m
VTEM Receiver	
Coil diameter	1.2 metre
Number of turns	100
Effective area	113.1 m^2
Sampling interval	0.1 s
Nominal terrain clearance	46 m
Magnetometer	
Type	Geometrics
Model	Optically pumped cesium vapour
Sensitivity	0.02 nT
Sampling interval	0.1 s
Cable length	12 m
Nominal terrain clearance	70 m
Radar Altimeter	
Type	Terra TRA 3000/TRI 40
Position	Beneath cockpit
Sampling interval	0.2 s
GPS navigation system	
Type	NovAtel
Model	WAAS enabled OEM4-G2-3151W
Antenna position	Helicopter tail
Sampling interval	0.2 s
Base Station Magnetometer/GPS	
Type	Geometrics
Model	Cesium vapour
Sensitivity	0.001 nT
Sampling interval	1 s

2.2. VTEM Configuration

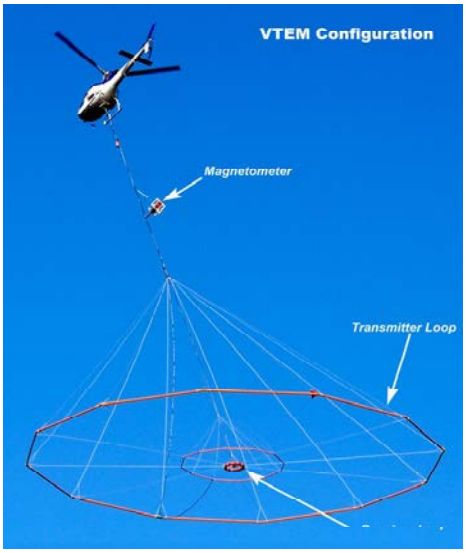

Configuration	
Cable angle with vertical	35 ˚
Cable length (EM receiver)	40 m
Cable length (Magnetometer)	12 m

2.3. VTEM decay sampling scheme

VTEM B-field System Decay Sampling scheme				
Array	Microseconds			
Index	Middle	Start	End	Width
8	83	78.1	88.5	10.4
9	99	88.6	109.4	20.8
10	120	109.4	130.2	20.8
11	141	130.2	151.0	20.8
12	167	151.1	182.3	31.2
13	198	182.3	213.5	31.2
14	234	213.6	255.2	41.6
15	281	255.2	307.3	52.1
16	339	307.3	369.8	62.5
17	406	369.8	442.7	72.9
18	484	442.7	526.0	83.3
19	573	526.1	619.8	93.7
20	682	619.8	744.8	125.0
21	818	744.8	890.6	145.8
22	974	890.6	1057.3	166.7
23	1151	1057.3	1244.8	187.5
24	1370	1244.8	1494.8	250.0
25	1641	1494.8	1786.5	291.7
26	1953	1786.5	2119.8	333.3
27	2307	2119.8	2494.8	375.0
28	2745	2494.8	2994.8	500.0
29	3286	2994.8	3578.1	583.3
30	3911	3578.1	4244.8	666.7
31	4620	4244.8	4994.8	750.0
32	5495	4994.8	5994.8	1000.0
33	6578	5994.8	7161.5	1166.7
34	7828	7161.5	8494.8	1333.3

2.4. VTEM Transmitter Waveform over one half-period (July 2010)

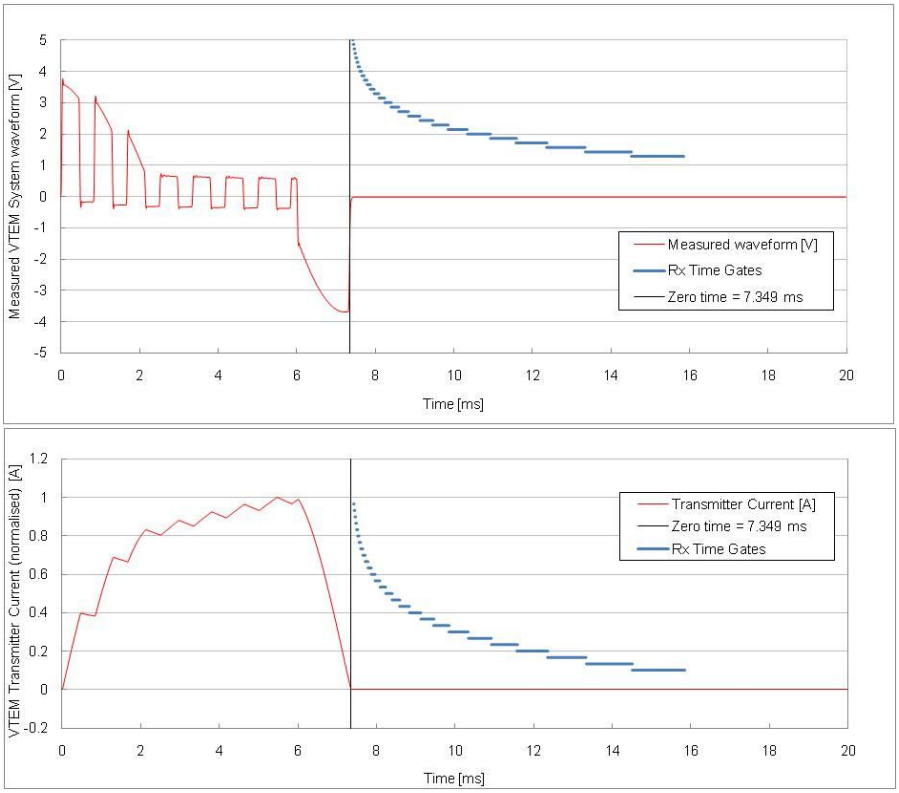

3. PROCESSING

3.1. Processing parameters

Coordinates	
Projection	Finland Uniform Coordinate System
Datum	KKJ
Spherics rejection (EM and Magnetic data)	
Non-linear filter	4 point
Non-linear filter sensitivity	0.0001
Low-pass filter wavelength	25 m
Lag correction of other sensors to EM receiver position	
GPS	16 m
Radar	26 m
Magnetometer	17 m

3.2. Flight Path

The flight path, recorded by the acquisition program as WGS 84 latitude/longitude, was converted into the UTM coordinate system in Oasis Montaj. The flight path was drawn using linear interpolation between x,y positions from the navigation system. Positions are updated every second and expressed as UTM eastings (x) and UTM northings (y).

3.3. Electromagnetic Data

A three stage digital filtering process was used to reject major sferic events and to reduce system noise. Local sferic activity can produce sharp, large amplitude events that cannot be removed by conventional filtering procedures. Smoothing or stacking will reduce their amplitude but leave a broader residual response that can be confused with geological phenomena. To avoid this possibility, a computer algorithm searches out and rejects the major sferic events.

The signal to noise ratio was further improved by the application of a low pass linear digital filter. This filter has zero phase shift which prevents any lag or peak displacement from occurring, and it suppresses only variations with a wavelength less than the specified filter wavelength.

3.4. Magnetic Data

The processing of the magnetic data involved the correction for diurnal variations by using the digitally recorded ground base station magnetic values. The base station magnetometer data was edited and merged into the Geosoft GDB database on a daily basis. The aeromagnetic data was corrected for diurnal variations by subtracting the observed magnetic base station deviations.

Tie line levelling was carried out by adjusting intersection points along the traverse lines. A micro-levelling procedure was then applied. This technique is designed to remove persistent low-amplitude components of flight-line noise remaining after tie line levelling.

The corrected magnetic data was interpolated between survey lines using a random point gridding method to yield x-y grid values for a standard grid cell size of a quarter of the line spacing. The Minimum Curvature algorithm was used to interpolate values onto a rectangular regular spaced grid.

3.5. Digital Terrain Model

Subtracting the radar altimeter data from the GPS elevation data creates a digital elevation model. To correct for minor elevation differences that are evident in this data when gridded, Shuttle Radar Topography Mission (SRTM) data have been used.

3.6. Decay Constant Channel

Confined conductors in a resistive host rock environment exhibit exponential decay at late times in the EM data. The decay constant (τ) of a conductor is defined as the time it will take for the measured response to decay to 1/e of the amplitude, i.e.:

$$EMF = Ae^{-t/\tau}$$

Taking the natural logarithm on both sides, this becomes:

$$\ln(EMF) = \ln(A) - t/\tau.$$

This is a straight line with slope (m) given by

$$m = -1/\tau.$$

The same relationship holds for EM data. Values for τ are found using semi-automated routine based on the following strategy: The EMF values are transformed to the logarithmic domain. A range of straight lines are fitted to all data channels above a specified noise level. The purpose is to determine which channels (if any) best approximate straight line behaviour in this domain. (In the case of a layered earth or homogenous half-space the EM response will be characterized by power-law decay and will not yield meaningful decay constants as defined above. These areas will appear as gaps on the tau grids.)

All possible combinations of channels are tested starting with the four channels. A first order polynomial least squares fit for channels one to four is calculated, followed by two to five, three to six, etc. Then the number of channels is increased by one and the process repeated, i.e. channels one to five are analyzed, followed by two to six, three to seven, etc. Only channel combinations to which a straight line can be fitted with least squares regression coefficient higher than 0.997 are allowed to be analyzed in the next phase. At this point the straight line slope associated with the highest number of channels occurring the latest in time, is used to calculate the decay constant for every station. These values are filtered (Low Pass Filter Cut-off: 30 m), gridded and presented as a contour map. Channels 30 to 35 were used for the tau channels.

It is important to note that decay constant peaks are associated with profile anomaly peaks and do not necessarily coincide with the exact conductor position.

4. DELIVERABLES

VTEM Survey and logistics report		
Format	PDF	
Copies	2 x Digital (DVD/CD) 2 x Hard copy	
Database		
Format	Digital Geosoft (.GDB)	
Channels	Name	Description
	X	X positional data (wgs)
	Y	Y positional data (wgs)
	Xkkj	X positional data (kkj)
	Ykkj	Y positional data (kkj)
	Lon	Longitude data
	Lat	Latitude data
	Z	GPS antenna elevation (metres above sea level)
	Radar	Helicopter terrain clearance from radar altimeter (metres above ground level)
	RxAlt	EM Receiver and Transmitter terrain clearance (metres above ground level)
	DTM	Digital terrain model (metres)
	Gtime	UTC time (seconds of the day)
	MagTF	Raw Total Magnetic field data (nT)
	MagBase	Magnetic diurnal variation data (nT)
	MagDiu	Total Magnetic field diurnal variation and lag corrected data (nT)
	MagTieL	Tie-line leveled Total Magnetic field data (nT)
	MagMicL	Microleveled Total Magnetic field data (nT)
	dBdtZ[8] to dBdtZ[34]	dB/dtZ, Time Gates 83 µs to 7828 µs (pV/A/m^4)
	dBdtX[14] to dBdtX[34]	dB/dtX, Time Gates 234 µs to 7828 µs (pV/A/m^4)
	dBdtX_FF[14] to dBdtX_FF[34]	Fraser Filter dB/dtX, Time Gates 234 µs to 78285 µs (pV/A/m^4)
	dBdtX_SFF_15_25	Stacked Fraser Filtered data from channel 15 to 25 (pV/A/m^4)
	BfieldZ[8] to BfieldZ[34]	B-fieldZ, Time Gates 83 µs to 7828 µs (pV.ms/A/m^4)
	BfieldX[14] to BfieldX[34]	B-fieldX, Time Gates 234 µs to 7828 µs (pV.ms/A/m^4)
	BfieldX_FF[14] to BfieldX_FF[34]	Fraser Filtered B-fieldX, Time Gates 234 µs to 7828 µs (pV.ms/A/m^4)
	BfieldX_SFF_15_25	Stacked Fraser Filtered data from channel 15 to 25 (pV.ms/A/m^4)
	dBdtZ_Tau	dBdt Decay Constant, Time Gates 3911 µs to 7828 µs (ms)
	BfieldZ_Tau	Bfield Decay Constant, Time Gates 3911 µs to 7828 µs (ms)
	PLM	Power line monitor

Grids		
Format	Digital Geosoft (.GRD and .GI)[1]	
Grids	Name	Description
	A806_Mag	Total Magnetic field (nT)
	A806_dBdtX_SFF	dBdtX Stacked Fraser Filtered data
	A806_BfieldX_SFF	BfieldX Stacked Fraser Filtered data

Maps		
Format	Digital Geosoft (.MAP)	
Scale	1:50 000	
Maps	Name	Description
	A806_Mag	Total Magnetic field colour contours
	A806_dBdtZ_Log	VTEM dB/dtZ profiles, Time Gates 0.234 – 7.828 ms in linear - logarithmic scale
	A806_dBdtX_SFF	dBdtX Stacked Fraser Filtered data
	A806_BfieldZ_Log	VTEM B-fieldZ profiles, Time Gates 0.234 – 7.828 ms in linear - logarithmic scale
	A806_BfieldX_SFF	BfieldX Stacked Fraser Filtered data

Waveform		
Format	Digital Excel Spreadsheet (A806_VTEM_Waveform.xls)	
Columns	Name	Description
	Time	Sampling rate interval, 10.416 µs
	Volt	Output voltage of the receiver coil (volt)
	Current	Transmitter current (normalised to 1A peak)

Google Earth Flight Path file	
Format	Google Earth A806_FlightPath.kmz
	Free version of Google Earth software can be downloaded from, http://earth.google.com/download-earth.html

[1] A Geosoft .GRD file has a .GI metadata file associated with it, containing grid projection information.

5. PERSONNEL

Geotech Airborne Limited Personnel	
Crew chief/ Operator	Hermann Mueller
Data Processing (Preliminary)	Lawrence Guta
Data Processing (Final) /Reporting	Matt Holbrook
Final data supervision	Malcolm Moreton Data Processing Manager (malcolm@geotechairborne.com)
Overall project management	Keith Fisk Managing Partner and Director (keith@geotechairborne.com)

APPENDIX A

GENERALIZED MODELING RESULTS OF THE VTEM SYSTEM (by Roger Barlow)

Introduction

The VTEM system is based on a concentric or central loop design, whereby, the receiver is positioned at the centre of a 26.1 metres diameter transmitter loop that produces a dipole moment up to 625,000 NIA at peak current. The wave form is a bi-polar, modified square wave with a turn-on and turn-off at each end. With a base frequency of 25 Hz, the duration of each pulse is approximately 7.5 milliseconds followed by an off time where no primary field is present.

During turn-on and turn-off, a time varying field is produced (dB/dt) and an electro-motive force (emf) is created as a finite impulse response. A current ring around the transmitter loop moves outward and downward as time progresses. When conductive rocks and mineralization are encountered, a secondary field is created by mutual induction and measured by the receiver at the centre of the transmitter loop.

Measurements are made during the off-time, when only the secondary field (representing the conductive targets encountered in the ground) is present.

Efficient modeling of the results can be carried out on regularly shaped geometries, thus yielding close approximations to the parameters of the measured targets. The following is a description of a series of common models made for the purpose of promoting a general understanding of the measured results.

Variation of Plate Depth

Geometries represented by plates of different strike length, depth extent, dip, plunge and depth below surface can be varied with characteristic parametres like conductance of the target, conductance of the host and conductivity/thickness and thickness of the overburden layer.

Diagrammatic models for a vertical plate are shown in figures A and G at two different depths, all other parametres remaining constant. With this transmitter-receiver geometry, the classic **M** shaped response is generated. Figure A shows a plate where the top is near surface. Here, amplitudes of the duel peaks are higher and symmetrical with the zero centre positioned directly above the plate. Most important is the separation distance of the peaks. This distance is small when the plate is near surface and widens with a linear relationship as the plate (depth to top) increases. Figure G shows a much deeper plate where the separation distance of the peaks is much wider and the amplitudes of the channels have decreased.

Variation of Plate Dip

As the plate dips and departs from the vertical position, the peaks become asymmetrical. Figure B shows a near surface plate dipping 80º. Note that the direction of dip is toward the high shoulder of the response and the top of the plate remains under the centre minimum.

As the dip increases, the aspect ratio (Min/Max) decreases and this aspect ratio can be used as an empirical guide to dip angles from near 90º to about 30º. The method

is not sensitive enough where dips are less than about 30º. Figure E shows a plate dipping 45º and, at this angle, the minimum shoulder starts to vanish. In Figure D, a flat lying plate is shown, relatively near surface. Note that the twin peak anomaly has been replaced by a symmetrical shape with large, bell shaped, channel amplitudes which decay relative to the conductance of the plate.

Figure H shows a special case where two plates are positioned to represent a synclinal structure. Note that the main characteristic to remember is the centre amplitudes are higher (approximately double) compared to the high shoulder of a single plate. This model is very representative of tightly folded formations where the conductors where once flat lying.

Variation of Prism Depth

Finally, with prism models, another algorithm is required to represent current on the plate. A plate model is considered to be infinitely thin with respect to thickness and incapable of representing the current in the thickness dimension. A prism model is constructed to deal with this problem, thereby, representing the thickness of the body more accurately.

Figures C, F and I show the same prism at increasing depths. Aside from an expected decrease in amplitude, the side lobes of the anomaly show a widening with deeper prism depths of the bell shaped early time channels.

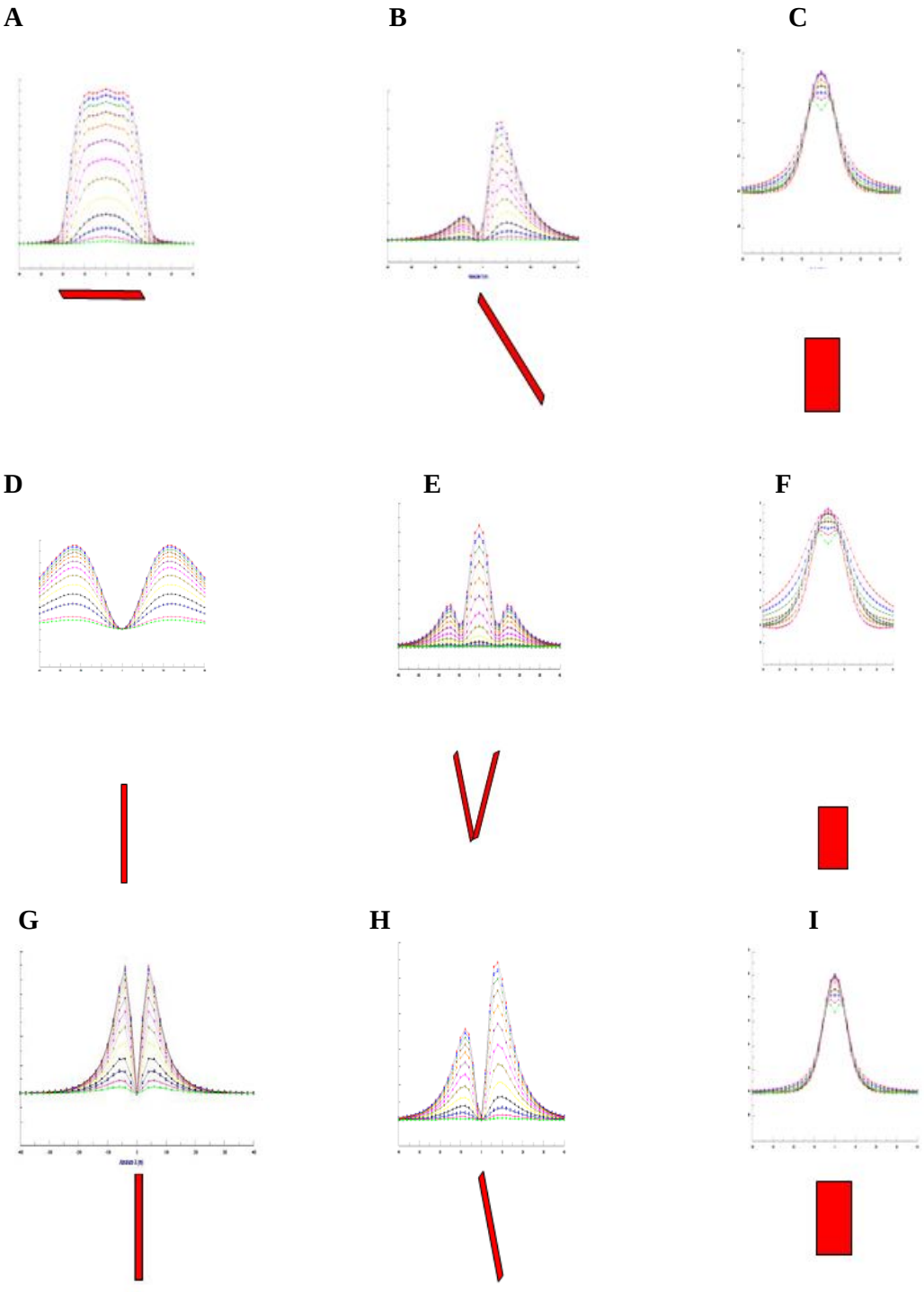
A
B
C
D
E
F
G
H
I

General Modeling Concepts

A set of models has been produced for the Geotech VTEM® system with explanation notes (see models A to I above). The reader is encouraged to review these models, so as to get a general understanding of the responses as they apply to survey results. While these models do not begin to cover all possibilities, they give a general perspective on the simple and most commonly encountered anomalies.

When producing these models, a few key points were observed and are worth noting as follows:

- For near vertical and vertical plate models, the top of the conductor is always located directly under the centre low point between the two shoulders in the classic **M** shaped response.
- As the plate is positioned at an increasing depth to the top, the shoulders of the **M** shaped response, have a greater separation distance.
- When faced with choosing between a flat lying plate and a prism model to represent the target (broad response) some ambiguity is present and caution should be exercised.
- With the concentric loop system and Z-component receiver coil, virtually all types of conductors and most geometries are most always well coupled and a response is generated (see model H). Only concentric loop systems can map this type of target.

The modelling program used to generate the responses was prepared by PetRos Eikon Inc. and is one of a very few that can model a wide range of targets in a conductive half space.

General Interpretation Principals

Magnetics

The total magnetic intensity responses reflect major changes in the magnetite and/or other magnetic minerals content in the underlying rocks and unconsolidated overburden. Precambrian rocks have often been subjected to intense heat and pressure during structural and metamorphic events in their history. Original signatures imprinted on these rocks at the time of formation have, it most cases, been modified, resulting in low magnetic susceptibility values.

The amplitude of magnetic anomalies, relative to the regional background, helps to assist in identifying specific magnetic and non-magnetic rock units (and conductors) related to, for example, mafic flows, mafic to ultramafic intrusives, felsic intrusives, felsic volcanics and/or sediments etc. Obviously, several geological sources can produce the same magnetic response. These ambiguities can be reduced considerably if basic geological information on the area is available to the geophysical interpreter.

In addition to simple amplitude variations, the shape of the response expressed in the wave length and the symmetry or asymmetry, is used to estimate the depth, geometric parameters and magnetization of the anomaly. For example, long narrow magnetic linears usually reflect mafic flows or intrusive dyke features. Large areas with complex magnetic patterns may be produced by intrusive bodies with significant magnetization, flat lying magnetic sills or sedimentary iron formation. Local isolated circular magnetic patterns often represent plug-like igneous intrusives such as kimberlites, pegmatites or volcanic vent areas.

Because the total magnetic intensity (TMI) responses may represent two or more closely spaced bodies within a response, the second derivative of the TMI response may be helpful for distinguishing these complexities. The second derivative is most useful in mapping near surface linears and other subtle magnetic structures that are partially masked by nearby higher amplitude magnetic features. The broad zones of higher magnetic amplitude, however, are severely attenuated in the vertical derivative results. These higher amplitude zones reflect rock units having strong magnetic susceptibility signatures. For this reason, both the TMI and the second derivative maps should be evaluated together.

Theoretically, the second derivative, zero contour or colour delineates the contacts or limits of large sources with near vertical dip and shallow depth to the top. The vertical gradient map also aids in determining contact zones between rocks with a susceptibility contrast, however, different, more complicated rules of thumb apply.

Concentric Loop EM Systems

Concentric systems with horizontal transmitter and receiver antennae produce much larger responses for flat lying conductors as contrasted with vertical plate-like conductors. The amount of current developing on the flat upper surface of targets having a substantial area in this dimension, are the direct result of the effective coupling angle, between the primary magnetic field and the flat surface area. One therefore, must not compare the amplitude/conductance of responses generated from flat lying bodies with those derived from near vertical plates; their ratios will be quite different for similar conductances.

Determining dip angle is very accurate for plates with dip angles greater than 30º. For angles less than 30º to 0º, the sensitivity is low and dips can not be distinguished accurately in the presence of normal survey noise levels.

A plate like body that has near vertical position will display a two shoulder, classic **M** shaped response with a distinctive separation distance between peaks for a given depth to top.

It is sometimes difficult to distinguish between responses associated with the edge effects of flat lying conductors and poorly conductive bedrock conductors. Poorly conductive bedrock conductors having low dip angles will also exhibit responses that may be interpreted as surfacial overburden conductors. In some situations, the conductive response has line to line continuity and some magnetic correlation providing possible evidence that the response is related to an actual bedrock source.

The EM interpretation process used, places considerable emphasis on determining an understanding of the general conductive patterns in the area of interest. Each area has different characteristics and these can effectively guide the detailed process used.

The first stage is to determine which time gates are most descriptive of the overall conductance patterns. Maps of the time gates that represent the range of responses can be very informative.

Next, stacking the relevant channels as profiles on the flight path together with the second vertical derivative of the TMI is very helpful in revealing correlations between the EM and Magnetics.

Next, key lines can be profiled as single lines to emphasize specific characteristics of a conductor or the relationship of one conductor to another on the same line. Resistivity Depth sections can be constructed to show the relationship of conductive overburden or conductive bedrock with the conductive anomaly.

APPENDIX B

VTEM X-COMPONENT DATA

1. X COIL DATA

1.1. Sign convention

VTEM's X component data produces crossover type anomalies. This is unlike the Z component of maxima or minima above conductors. During acquisition the convention is for X coil data to be positive in the direction of flight. In the processing phase the polarity is adjusted to follow the right hand rule for multi-component transient electromagnetic methods.

For N-S lines the sign convention for the X in-line component crossover is positive-negative pointing south to north for vertical plate conductors perpendicular to the profile. For E-W lines the sign convention for the X in-line component crossover is positive-negative pointing west to east for vertical plate conductors perpendicular to the profile. X component data for alternating/opposite flight directions are reversed (multiplied by negative one) in the final database to account for this polarity convention.

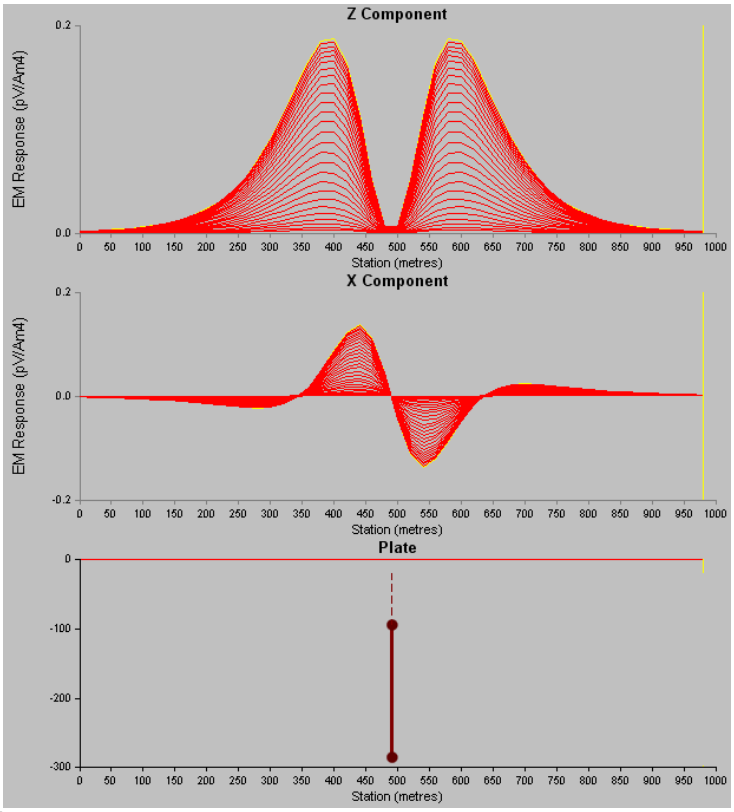

Figure 1: Z- and X-component responses over vertical plate conductor indicating sign convention for X component data.

1.2. Fraser Filter and Stacked Fraser Filter

The Fraser Filter converts crossovers of the correct polarity into peak responses of X component by differencing successive values. It is calculated as $(f_1+f_2)-(f_3+f_4)$ where f_i are data from four consecutive stations. This is a derivative filter and likely to increase any noise in data.

A useful presentation of X-component data is the Staked Fraser Filter. The Stacked Fraser Filter data are calculated as the average value of 11 channels (15 to 25) of Fraser Filtered X-component data. The signal to noise ratio is improved and information from 11 channels are combined into one, which allows easier presentation in grid or map format.

1.3. Effect of loop tilt

Whenever the X coil is not aligned exactly vertical, it also measures a part of the Z-component response. When the Z-component response is much larger in amplitude than the X-component response it can dominate the measured X-component data. This becomes especially evident when line polarities are reversed; true X-component responses would be coherent from line to line after polarity correction whereas the Z-component becomes alternating negative and positive responses. An example of this is shown in Fig. 2.

number. It is clear that the measured X-component is dominated by Z-component response.

Provided the tilt angle of the coil is known, a correction can be applied to the data. X coil tilt is not measured in with the VTEM system and an approximate procedure was developed to calculate tilt angles in the X-Z plane and remove the Z-component influence on the X-component data.

1.3.1 Quantifying the effect of loop tilt

With Z and X the real vector components and $\underline{Z}$ and $\underline{X}$ the measured components and α the tilt angle of the loop in the line direction, we have:

$$\underline{Z} = Z\cos(\alpha) + X\sin(\alpha)$$
$$\underline{X} = X\cos(\alpha) - Z\sin(\alpha)$$

Over half-space or layered earth environments X=0.

So that:

$$\underline{Z} = Z\cos(\alpha)$$
$$\underline{X} = -Z\sin(\alpha)$$

and

$$\alpha = \text{atan}(-\underline{X}/\underline{Z}).$$

Any value of $\underline{X}$ is therefore ascribed to the term $-Z\sin(\alpha)$. This is sometimes observed in VTEM data with measured X values being negative in general and following inverse trends from the Z-component data (Fig. 3).

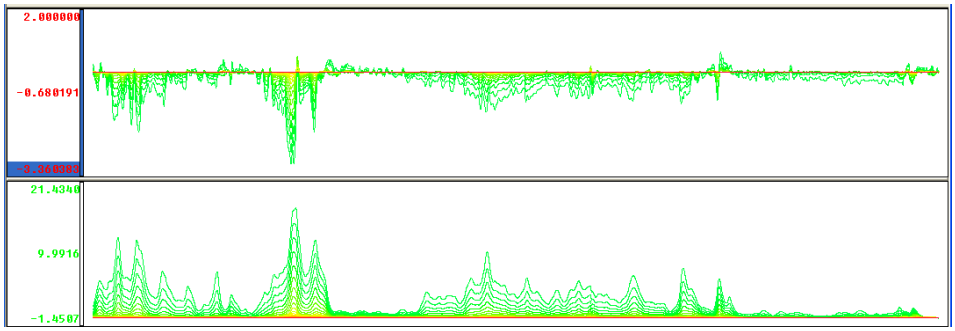

Figure 3: X-component (top) and Z-component (bottom) VTEM data.

1.3.2 Approximate calculation of loop tilt

The equation α=atan(-X/ Z) is used to calculate approximate tilt-angles at each position for all channels. An average tilt angle is calculated from channels 15 to 20 and filtered with:

Non-Linear filter: 100 fids; 0.2 sensitivity
LP filter: 500 fids.
(Parameters are determined empirically for individual data sets)

The filtering ensures that anomalous X responses are excluded from subsequent calculations, but also causes small errors in the correction factor. As a final step and average tilt angle (α) for each line is calculated.

1.3.3 Correcting X-component data

A new channel for X-component data is calculated as:

SLx_Angle_Corrected= X *cos(α)+Z *sin(α).

The results are to centre responses round zero and visually enhance the occurrences of X-component anomalies (Fig. 4).

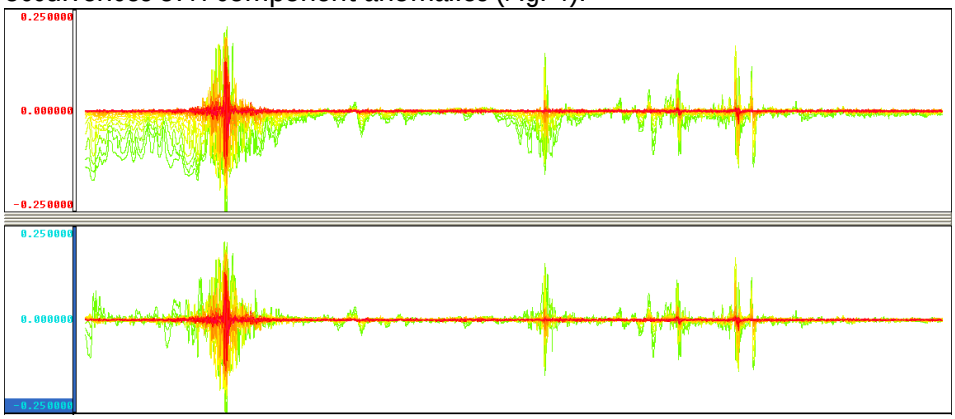

Figure 4: X-component data before (top) and after (bottom) approximate tilt correction.

As this is an approximate correction only, the corrected data might not give accurate results in quantitative modeling or inversions.

The results of the tilt correction and subsequent polarity corrections on gridded data are shown in Fig. 5. After the tilt correction the long wavelength similarities between X- and Z-coil data is no longer evident. The polarity correction now improves line-to-line continuity of as expected.

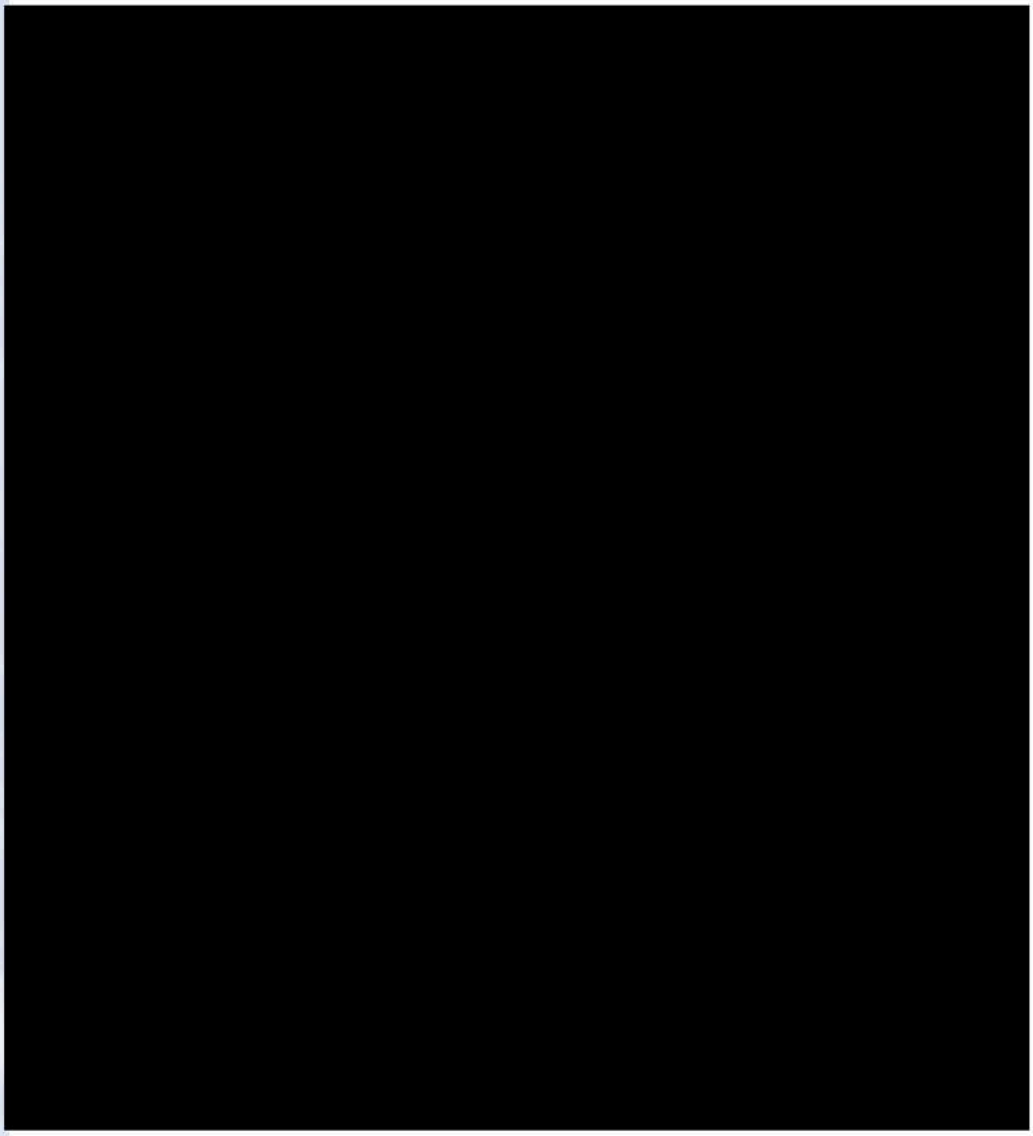

1.4. Typical X-component responses

Forward modeled X- and Z-component responses for some typical plate models in free air are provided below as reference. These were calculated with Maxwell software.

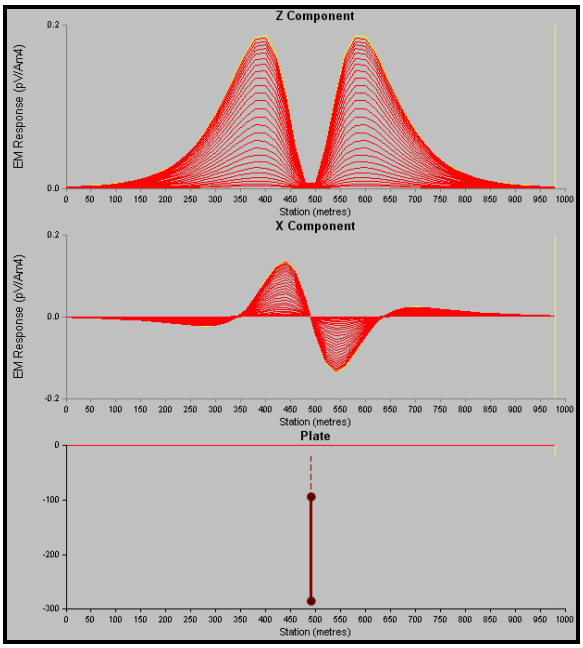

VERTICAL PLATE

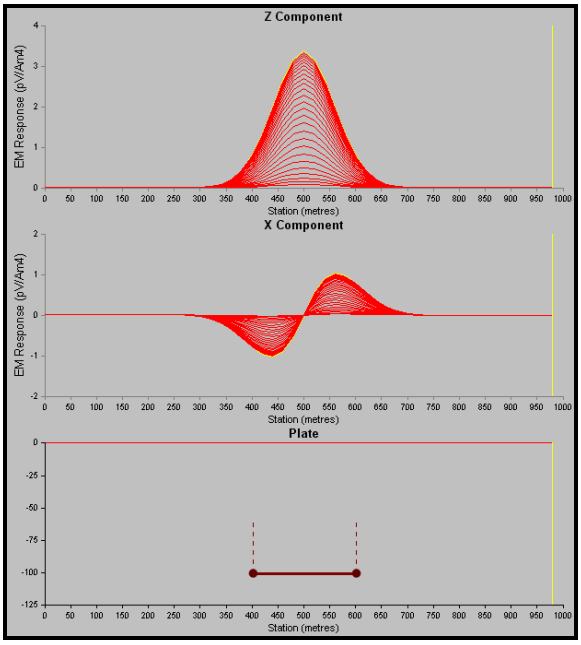

HORIZONTAL PLATE

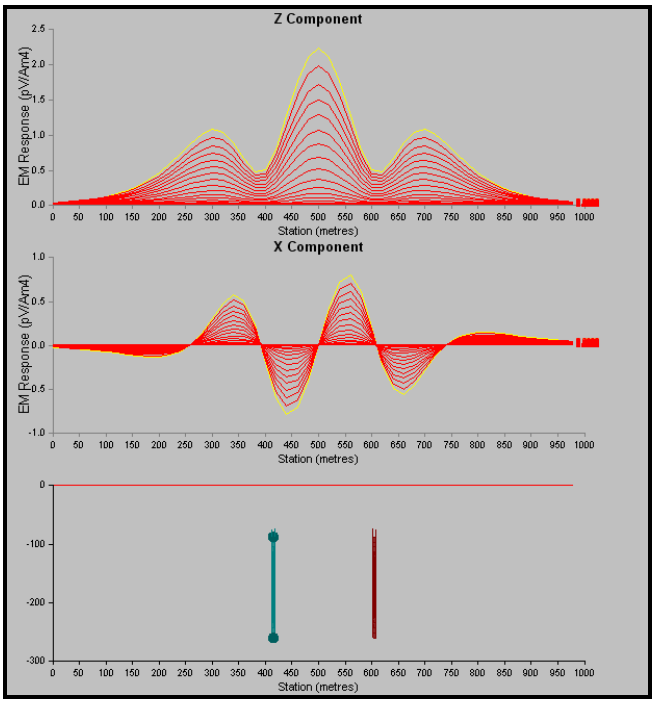

TWO VERTICAL PLATES 200m APART

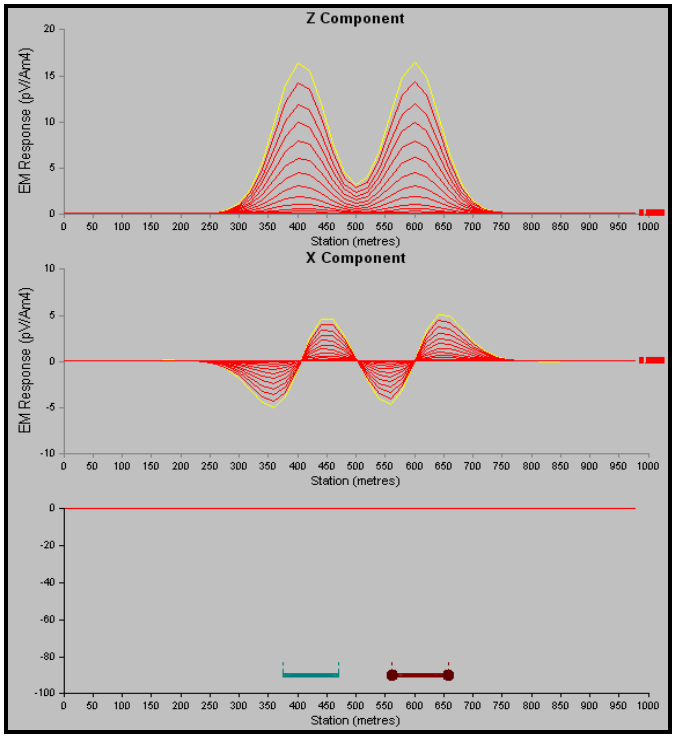

TWO HORIZONTAL PLATES; EDGES 100m APART

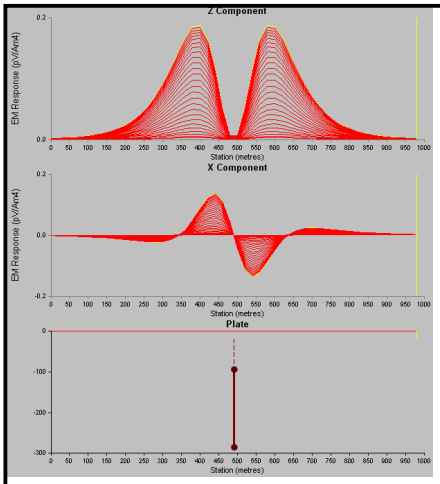

90 degrees

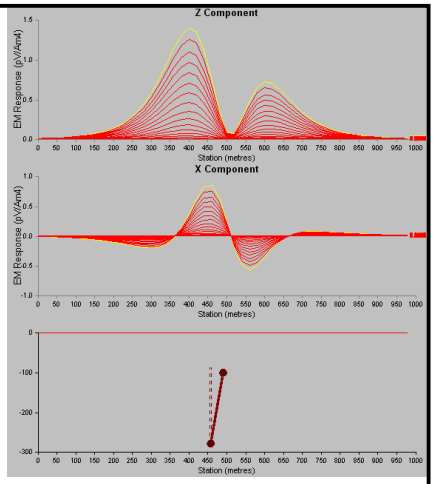

80 degrees

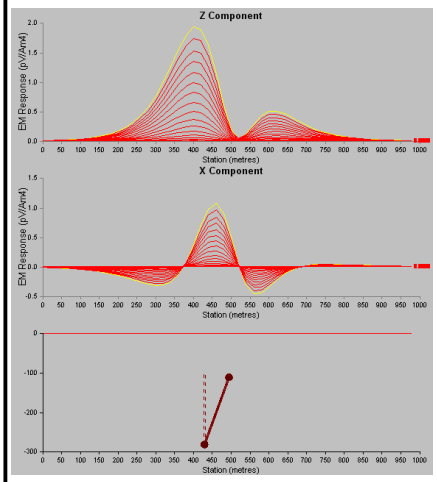

70 degrees

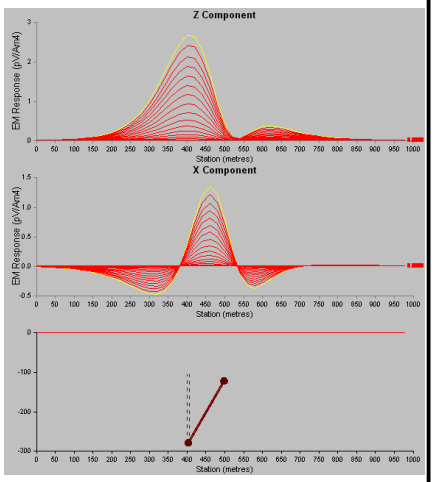

60 degrees

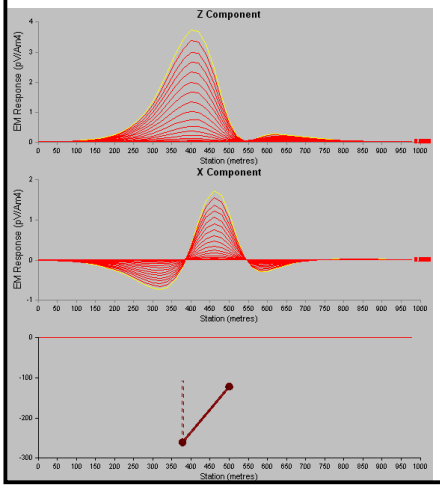

50 degrees

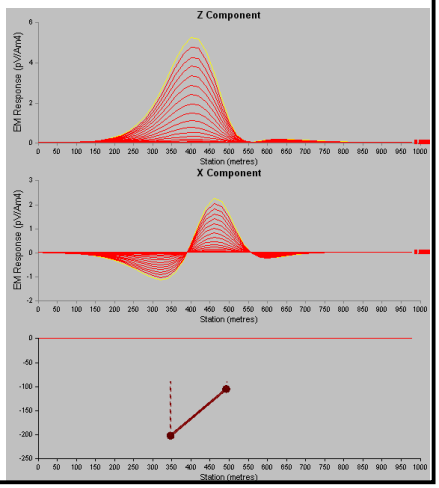

40 degrees

VARIATION WITH DIP

APPENDIX C

GEOPHYSICAL MAP IMAGES
(not to scale)